ELSEVIER

Solid State Ionics 144 (2001) 65–69

SOLID STATE IONICS

www.elsevier.com/locate/ssi

The $LiMn_2O_4$ to λ-MnO_2 phase transition studied by in situ neutron diffraction

Helena Berg [a], Håkan Rundlöv [b], John O. Thomas [a,*]

[a] *Materials Chemistry, Ångström Laboratory, Uppsala University, Box 538, SE-751 21 Uppsala, Sweden*
[b] *Studsvik Neutron Research Laboratory, SE-611 82 Nyköping, Sweden*

Received 17 April 2001; accepted 20 June 2001

Abstract

The $Li_xMn_2O_4$ to λ-MnO_2 phase transition, as lithium is extracted electrochemically from the spinel structure, has been studied by in situ neutron diffraction. The 'single-phase' composition around 4.1 V is found to be strongly dependent on potential, with the Li content (x) varying between 0.65(9) and 0.49(12). The amount of Li in the cubic λ-MnO_2 phase is 0.27(13) with cell parameter $a = 8.115(1)$ Å, in good agreement with earlier ex situ neutron diffraction results. A simple in situ neutron diffraction method is presented for following structural changes during electrochemical cycling of a lithium insertion compound.

Keywords: Lithium-ion battery; Spinel; In situ neutron diffraction

1. Introduction

Lithium manganese oxide ($LiMn_2O_4$) can undergo reversible extraction/insertion of lithium in the range ca. 3.8 to 4.2 V vs. Li/Li^+, thus rendering it a promising cathode material for rechargeable lithium-ion batteries [1–8]. It has the spinel structure, with Li and Mn in tetrahedral ($8a$) and octahedral ($16d$) positions, respectively, within a closed-packed array of oxygen atoms ($32e$ positions). A typical discharge curve for a $\langle LiMn_2O_4|$liq. el.$|Li\rangle$ cell is shown in Fig. 1.

The amount of cyclable lithium determines the reversible capacity of the material, and can be measured both electrochemically and crystallographically. In calculating lithium concentration from electrochemical measurements, it is generally assumed that all current passed through the cell can be related to the lithium extraction/insertion process. The amount of lithium in the structure can also be refined from neutron powder diffraction data, and it is common that results from the two methods differ. For example, the structure at the highest potential (ca. 4.5 V) is generally referred to as the λ-MnO_2 phase [4] and is assumed to be a lithium-free phase, while ex situ neutron diffraction shows that ca. 25% of the lithium remains in the structure [5]. This raises the question of the relationship between observed structure and electrochemical performance.

The lithium extraction process has been followed previously by in situ synchrotron X-ray diffraction [7,8]. The lithium content in the $Li_xMn_2O_4$ has been determined from the current passed through the cell.

* Corresponding author. Tel.: +46-18-4713763; fax: +46-18-513548.
E-mail address: josh.thomas@mkem.uu.se (J.O. Thomas).

0167-2738/01/$ - see front matter
PII: S0167-2738(01)00894-3

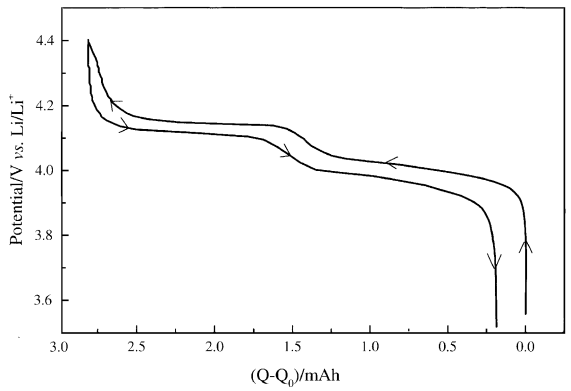

Fig. 1. A typical first-cycle charge/discharge curve for a $\langle LiMn_2O_4|liq.el.|Li\rangle$ cell.

The lithium extraction process from $LiMn_2O_4$ has here been studied by in situ neutron powder diffraction, using a novel electrochemical device modified especially for this purpose. The lithium content has been derived from Rietveld refinement.

2. Experimental

2.1. The electrochemical cell

The cell used was a modified version of that developed by Bergström et al. [9] (Fig. 2). A Pyrex© tube was lined with Li foil and sealed at each end with brass plugs. The lithium foil was then covered with a Celgard© separator. A cathode mixture (~ 5 g) composed of 60 wt.% $LiMn_2O_4$ (Danionics; made by solid-state reaction between Li_2CO_3 and MnO_2 at 725 °C), 37.5 wt.% electrolyte, and 2.5 wt.% carbon black was then placed inside the separator, and a current collector (a ca. 1-mm-diameter stainless-steel rod) was pressed into the cathode mixture along the tube axis. The electrolyte was a 1 M solution of $LiBF_4$ in 2:1 EC:DMC. Cells were assembled in a glove box under a dry argon atmosphere (< 2 ppm H_2O/O_2).

2.2. In situ neutron diffraction

The cell was sealed and charged at a constant current (1.0 mA) to the desired potentials. This corresponds to the very slow charge rate of ca. C/750. The potentials used were: 3.60 ('as prepared'), 4.00, 4.05, 4.10, 4.12, 4.16, and 4.24 V vs. Li/Li^+. Neutron diffraction data were collected at each potential at the steady-state medium-flux research reactor R2 in Studsvik, Sweden. A monochromator system with two copper crystals (220-reflection) was used in parallel alignment ($\lambda = 1.47$ Å). Diffractograms were collected at room temperature (295 K) in the 2θ range 4.00–139.92° in steps of 0.08°.

2.3. Structural refinement

Refinements of the $Li_xMn_2O_4$ data sets were based on the Rietveld method using the program FULLPROF [10,11]. The neutron scattering lengths used were Li: −1.90, Mn: −3.73 and O: 5.803 fm. The diffraction peaks were described by a pseudo-Voigt function; a Lorentzian contribution to the Gaussian peak shape was also refined. Peak asymmetry corrections were made for angles below 45° in 2θ. Background intensities were described by a linear interpo-

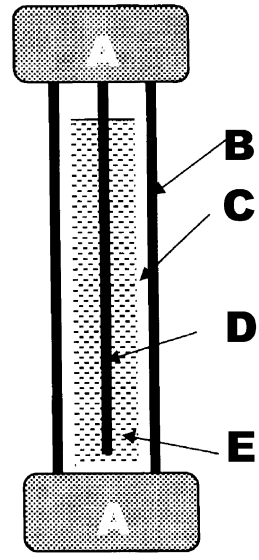

Fig. 2. A schematic representation of the cell used for in situ neutron diffraction studies: (A) brass plugs; (B) Pyrex© tube lined with lithium foil; (C) separator soaked in electrolyte; (D) current collector; (E) mixture of $LiMn_2O_4$, electrolyte and carbon black.

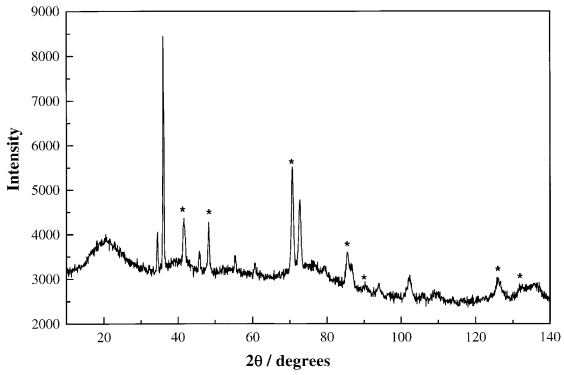

Fig. 3. Neutron diffraction profile from the whole cell. Peaks arising from the stainlees-steel current collector are marked with an asterisk (*).

lation between ca. 40 assumed background points. A lattice parameter and an atomic positional parameter for oxygen were refined together with a scale-factor and a 2θ zero-point parameter. The lithium content was also refined for the delithiated samples. Since occupancies and displacement parameters are correlated, the latter were fixed to the values obtained at 3.60 V ('as prepared').

The stainless-steel current collector also gave rise to diffraction peaks. These have been refined as two Fe phases, with strongly preferred orientations in the (100) and (110) directions, respectively. This was done in the refinements of the 'as prepared' data and then kept fixed in all subsequent refinements; only the scale factor for this contribution was included.

3. Results and discussion

The $LiMn_2O_4$ starting material was a single-phase powder with a lattice parameter of 8.221(1) Å, refined from neutron diffraction data [5]. Fig. 3 shows the diffraction profile from the cell in its uncharged state. Although the background is high (mainly incoherent scattering from the hydrogenous components in the electrolyte), the reflections are still well resolved. Data at the selected potentials have been refined, and the resulting parameters are summarised in Table 1. It is clear that the Mn–O framework remains intact during delithiation, and no additional peaks are observed. Lithium was found only at the $8a$ site, the same site as in the $LiMn_2O_4$ start material. The variation in the refined lattice parameter and lithium content in $Li_xMn_2O_4$ is plotted in Fig. 4. The lattice parameter is almost constant at potentials below 4.0 V, and falls rapidly between 4.0 and 4.1 V. There is anomalous behaviour in the lattice parameter at 4.16 V; it could be an experimental mishap for which we can find no explanation, or that some form of SEI layer starts to form at this potential. A more plausible explanation, however, could be that the abrupt upward shift in cell parameter is merely an artifact of an unresolved two-phase

Table 1
A summary of the refinement of in situ neutron diffraction data for $Li_xMn_2O_4$

Potential, V, vs. Li/Li^+	Uncharged	4.00	4.05	4.10	4.12	4.16	4.24
x in $Li_xMn_2O_4$ ($8a$ site)	1.0	1.0(1)	0.64(9)	0.65(9)	0.49(12)	0.22(16)	0.27(13)
Lattice parameter, a (Å)	8.225(1)	8.206(1)	8.155(1)	8.136(1)	8.113(1)	8.155(1)	8.155(1)
Oxygen coordinate, x_O	0.2647(3)	0.2644(3)	0.2641(3)	0.2637(3)	0.2633(3)	0.2653(4)	0.2632(3)
Temperature factor, B (Å^2)							
Li	1.7(1)	*	*	*	*	*	*
Mn	1.1(2)	*	*	*	*	*	*
O	0.8(1)	*	*	*	*	*	*
No. of background points	37	37	37	37	38	39	40
R_p (%)	1.94	1.56	1.73	1.66	1.97	1.60	1.59
R_{wp} (%)	2.68	1.95	2.17	2.10	3.03	2.09	1.99
χ^2	2.06	1.19	1.51	1.42	2.90	1.72	1.33

* Value fixed to that obtained from the refinement of the uncharged state.

system (with accompanying line broadening) with *a*-values of ca. 8.11 and 8.20 Å effectively superposed. It is also clear that the delithiation process begins at potentials above 4.0 V vs. Li/Li^+. From ex situ neutron diffraction studies, we know that the lithium content in the λ-MnO_2 phase is 0.28(5) [5]; this is reconfirmed by this present study. On the other hand, the lithium content for the 'single-phase' at ca. 4.10 V differs from earlier proposed compositions [7,12], where it was interpreted as a $Li_{0.5}Mn_2O_4$ phase, assuming that all current passed through the cell could be attributed to lithium extraction. However, the composition is strongly dependent on the voltage. The single-phase region is found between 4.05 and 4.14 V (Fig. 5), and the lithium content in the 8*a* sites decreases from 0.65 to 0.50 in this region.

Both in situ Raman [13] and in situ XRD [7,8] measurements have shown that $Li_xMn_2O_4$ passes through a two-phase region on its way to becoming the single-phase λ-MnO_2. This two-phase region is found in the $0.5 < x < 0.13$ range according to Ref. [14], and $0.45 < x < 0.20$ according to Ref. [8]. These *x*-values are calculated on the basis of current passed, assuming that the *x*-value decreases uniformly during the charge process. In the present study, no two-phase behaviour was detectable in the high potential region. This can be a result of the very slow charging rate used [7].

XPS studies have shown that some type of solid layer is formed on the surface of the cathode particles [15], somewhat reminiscent of the SEI-layer formed on a graphite anode [16]. A possible explanation for the discrepancies in the results is then that some of the charge passed is consumed during the formation of such a layer.

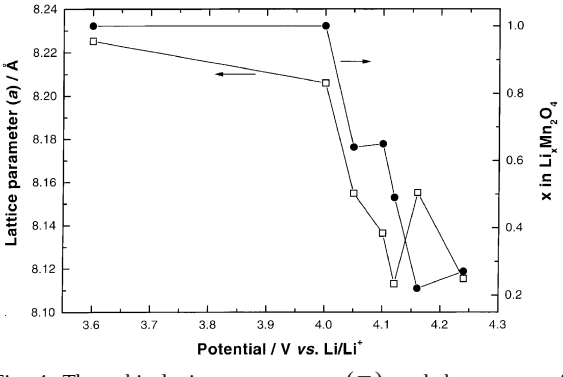

Fig. 4. The cubic lattice parameter, *a* (□), and the amount of lithium, *x* (●), $Li_xMn_2O_4$ plotted as a function of cell potential, *V*.

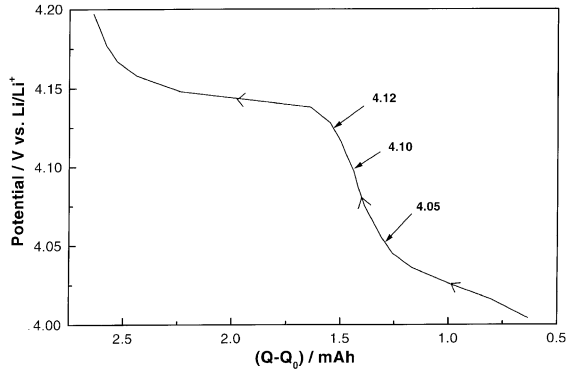

Fig. 5. A detailed plot of the charge curve for a $\langle LiMn_2O_4|liq.el.|Li\rangle$ cell.

3.1. A final comment

The lithium content in $Li_xMn_2O_4$ has, thus, been followed (for the first time) by in situ neutron diffraction as a function of cell potential. The method used is simple and the lithium content obtained from these refinements is in agreement with that refined earlier from ex situ neutron diffraction measurements [5]. Compared to ex situ studies, the in situ method has the advantage of using only one cell, but the large amount of active material involved means that much longer equilibration times are needed.

Acknowledgements

This work was supported by The Swedish Natural Science Research Council (NFR), The Swedish Energy Authority (STEM), the EU (Joule III) Programme, and The Foundation for Environmental Strategic Research (MISTRA). All are hereby gratefully acknowledged. Thanks are also due to Ami Andersson (Uppsala University) for many fruitful discussions concerning the cell preparation.

References

[1] R. Koksbang, J. Baker, H. Shi, M.Y. Saïdi, Solid State Ionics 84 (1996) 1.
[2] M.M. Thackeray, Prog. Solid State Chem. 25 (1997) 1.
[3] M. Winter, J.O. Besenhard, M.E. Spahr, P. Novàk, Adv. Mater. 10 (1998) 725.
[4] J.C. Hunter, J. Solid State Chem. 39 (1981) 142.
[5] H. Berg, J.O. Thomas, Solid State Ionics 126 (1999) 227.
[6] A. Blyr, C. Sigala, G. Amatucci, D. Guyomard, Y. Chabre, J.M. Tarascon, J. Electrochem. Soc. 145 (1998) 194.
[7] X.Q. Yang, X. Sun, S.J. Lee, J. McBreen, S. Mukerjee, M.L. Daroux, X.K. Xing, Electrochem. Solid-State Lett. 2 (1999) 157.
[8] S. Mukerjee, T.R. Thurston, N.M. Jisrawi, X.Q. Yang, J. McBreen, M.L. Daroux, X.K. Xing, J. Electrochem. Soc. 145 (1998) 466.
[9] Ö. Bergström, A.M. Andersson, K. Edström, T. Gustafsson, J. Appl. Cryst. 31 (1998) 823.
[10] H.M. Rietveld, J. Appl. Cryst. 2 (1969) 65.
[11] J. Rodriguez-Carjaval, ILL Internal Report, (1993) ILL, Grenoble, France.
[12] W. Liu, K. Kowal, G.C. Farrington, J. Electrochem. Soc. 145 (1998) 459.
[13] W. Huang, R. Frech, J. Power Sources 81–82 (1999) 616.
[14] K. Kanamura, H. Naito, T. Yao, Z. Takehara, J. Mater. Chem. 6 (1996) 33.
[15] T. Eriksson, T. Gustafsson, J.O. Thomas, Proc. Electrochem. Soc. 98-16 (1999) 315.
[16] P. Arora, R.E. White, M. Doyle, J. Electrochem. Soc. 145 (1998) 3647.